

# Potential and limitations of nucleon transfer experiments with radioactive beams at REX-ISOLDE

C. Gund<sup>1,a</sup>, H. Bauer<sup>1,b</sup>, J. Cub<sup>2,c</sup>, A. Dietrich<sup>1,d</sup>, T. Härtlein<sup>1,e</sup>, H. Lenske<sup>3</sup>, D. Pansegrau<sup>1,f</sup>, A. Richter<sup>2</sup>, H. Scheit<sup>1,g</sup>, G. Schrieder<sup>2</sup>, and D. Schwalm<sup>1</sup>

<sup>1</sup> Max-Planck-Institut für Kernphysik, D-69117 Heidelberg, Germany

<sup>2</sup> Institut für Kernphysik, Technische Universität Darmstadt, D-64298 Darmstadt, Germany

<sup>3</sup> Institut für Theoretische Physik, Universität Gießen, D-35392 Gießen, Germany

Received: 9 October 2000

Communicated by J. Äystö

**Abstract.** As a tool for studying the structure of nuclei far off stability the technique of  $\gamma$ -ray spectroscopy after low-energy single-nucleon transfer reactions with radioactive nuclear beams in inverse kinematics was investigated. Modules of the MINIBALL germanium array and a thin position-sensitive parallel plate avalanche counter (PPAC) to be employed in future experiments at REX-ISOLDE were used in a test experiment performed with a stable  $^{36}\text{S}$  beam on deuteron and  $^9\text{Be}$  targets. It is demonstrated that the Doppler broadening of  $\gamma$  lines detected by the MINIBALL modules is considerably reduced by exploiting their segmentation, and that for beam intensities up to  $10^6$  particles/s the PPAC positioned around zero degrees with respect to the beam axis allows not only to significantly reduce the  $\gamma$  background by requiring coincidences with the transfer products but also to control the beam and its intensity by single particle counting. The predicted large neutron pickup cross-sections of neutron-rich light nuclei on  $^2\text{H}$  and  $^9\text{Be}$  targets at REX-ISOLDE energies of  $2.2\text{ MeV}\cdot\text{A}$  are confirmed.

**PACS.** 29.40.Cs Gas-filled counters: ionization chambers, proportional, and avalanche counters – 29.30.Kv X- and  $\gamma$ -ray spectroscopy – 25.60.Je Transfer reactions

## 1 Introduction

REX-ISOLDE [1], an experiment presently constructed at the ISOLDE facility at CERN, is scheduled to supply beams of exotic nuclei with energies of up to  $2.2\text{ MeV}\cdot\text{A}$  starting in 2001. At these energies Coulomb excitation and transfer reactions in inverse kinematics on light target materials can be used to investigate the collective and single-particle structure of low-lying levels of nuclei with extreme  $N/Z$  ratios.

REX-ISOLDE uses the  $60\text{ keV } 1^+$  beams delivered by the ISOLDE facility and accelerates them to  $2.2\text{ MeV}\cdot\text{A}$  using a novel acceleration scheme employing a buncher-

trap, a charge-breeder, an intermediate mass-selector and three RF accelerator units. While for isotopes close to stability beam intensities of up to  $I = 10^{10}$  particles/s can be expected, the intensities decline rapidly as one approaches the neutron or proton dripline (e.g.,  $I(^{24}\text{Na}) \approx 5 \cdot 10^8\text{ s}^{-1}$ ,  $I(^{31}\text{Na}) \approx 50\text{ s}^{-1}$ ).

These low beam intensities require experimental setups optimized to achieve both high reaction rates and high detection efficiencies without compromising resolution. Since for particle spectroscopy thin targets and high-resolution spectrometers are needed, which usually have only small angular acceptances, counting rates will be low in such experiments. In contrast,  $\gamma$ -ray spectroscopy with a highly efficient germanium detector array offers the possibility to use thicker targets while maintaining excellent resolution. However, in experiments at low beam intensities the background  $\gamma$ -rays usually outnumber the nuclear reaction  $\gamma$ -rays by orders of magnitude, a problem which is even more pronounced when radioactive beams are used due to the  $\beta$ -decay background. It is therefore advantageous to detect at least one charged particle produced in the reaction in a large solid angle and to require a time coincidence with the  $\gamma$ -ray to achieve a sufficient background suppression. The most favorable approach for inverse reactions on very light target materials like  $^2\text{H}$  and at low

<sup>a</sup> Present address: Fraunhofer IIS-B, D-91058 Erlangen, Germany.

<sup>b</sup> Present address: McKinsey & Company, D-80538 München, Germany.

<sup>c</sup> Present address: DePfa Systems GmbH, D-55122 Mainz, Germany.

<sup>d</sup> Present address: Fachbereich Materialwissenschaft, Technische Universität Darmstadt, D-64287 Darmstadt, Germany.

<sup>e</sup> Present address: SAP AG, 69190 Walldorf, Germany.

<sup>f</sup> Present address: Robert Bosch GmbH, 70442 Stuttgart, Germany.

<sup>g</sup> e-mail: heiko.scheit@mpi-hd.mpg.de

beam intensities is to detect the heavy reaction product, whose momentum hardly differs from the momentum of the beam particle. Thus the heavy reaction products can easily be detected within their full solid angle by a detector positioned around zero degrees with respect to the beam axis. Alternatively, the detection of the beam particle in front of the target is possible, yet this would cause an extra energy loss of the beam before it reaches the target.

$\gamma$ -ray spectroscopy at low beam intensities requires a germanium array with excellent photopeak efficiency. As in REX-ISOLDE mainly low-lying levels of exotic nuclei will be investigated, the  $\gamma$  cascades are expected to be of low multiplicity. It is therefore possible to achieve the high efficiency by placing the germanium detectors very close to the target, which results in a considerable cost reduction per percent efficiency as only a moderate number of germanium modules is required. Yet, the close geometry has an important disadvantage. The large recoil velocities cause a considerable Doppler broadening of the  $\gamma$  lines as the width of a Doppler broadened peak increases with the solid angle covered by a single detector module. Internal segmentation of the modules is the best remedy for this problem as this does not sacrifice photopeak efficiency.

MINIBALL [2], a germanium array which was especially developed for low-multiplicity, high-efficiency  $\gamma$ -ray spectroscopy experiments will thus be used at REX-ISOLDE. Extrapolating from the measured efficiencies for a single module, MINIBALL will have a  $4\pi$  efficiency of about 15.5% at 646 keV and 12.5% at 1333 keV. For the individual MINIBALL modules the encapsulation technique and the semi-hexaconical shape of the EUROBALL modules [3] were employed, and with a length of 78 mm and a front diameter of 68 mm they are also of equal size. However, the MINIBALL modules are electrically segmented into six parts (see inset in fig. 3), which results in a six-fold enhanced granularity. In the experiment described below, standard electronics for the energy readout of the core and the six segments were used and only for the current signal of the core a pulse shape analysis was possible. New electronics for the MINIBALL array are presently commissioned, which will allow pulse shape analysis of the charge signals of both the core and the six segments while maintaining excellent energy resolution. With the aid of these electronics and advanced algorithms [4,5] to analyze the charge signals an improvement of the module granularity of one order of magnitude [4] can be achieved as compared to that of the six-fold segmented module without pulse shape analysis.

Pioneering work using reaccelerated radioactive nuclear beams together with  $\gamma$  spectroscopy was done at Leuven [6,7], where a high intensity  $^{19}\text{Ne}$  beam was used on a  $^{40}\text{Ca}$  target as well as on proton and deuteron targets. In order to show the feasibility of  $\gamma$ -ray spectroscopy experiments using inverse transfer reactions with very low-intensity beams at REX-ISOLDE beam energies a test experiment was performed at the tandem accelerator facility of the Max-Planck-Institut für Kernphysik, Heidelberg. In the measurement  $^{36}\text{S}$  beams at the maximum REX-ISOLDE energy of 2.2 MeV·A and with intensities

as low as  $2 \cdot 10^5$  particles/s were used together with targets of deuterium-enriched polythene and  $^9\text{Be}$ . For the deuterium target both proton and neutron pickup reactions were expected to take place, whereas only neutron pickup is expected using a beryllium target, as here the proton transfer is kinematically suppressed.

One aim of the experiment was to verify the predicted high transfer cross-sections for single neutron transfer at REX-ISOLDE beam energies [8]. The second aim was to determine the  $\gamma$ -energy resolution after Doppler correction for the MINIBALL modules under realistic conditions. Furthermore, it was aimed to examine how the few reaction  $\gamma$ -rays expected in low beam-intensity experiments can be effectively separated from the background. For this purpose the new REX-ISOLDE Parallel Plate Avalanche Counter (PPAC) [9] was mounted under zero degrees with respect to the beam to detect the heavy transfer products and to produce a reference signal for particle- $\gamma$  coincidence measurements.

## 2 Inverse reaction kinematics and differential cross-sections

In this section the test reaction of  $^{36}\text{S}$  on  $^2\text{H}$  and  $^9\text{Be}$  at a beam energy of 2.2 MeV·A is used to exemplify the kinematics of a typical inverse transfer reaction to be studied at REX-ISOLDE.

Since neutrons are not available as a target material, stable nuclei which have a weakly bound neutron should be used in neutron pickup experiments. Mainly two light target materials are available, which permit neutron-transfer reactions in inverse reaction kinematics at REX-ISOLDE energies: deuterium and beryllium. As the deuteron consists of a proton and a neutron bound with an energy of 2.2 MeV, besides the neutron pickup channel  $^2\text{H}(^{36}\text{S},^{37}\text{S})\text{p}$ , the proton pickup channel  $^2\text{H}(^{36}\text{S},^{37}\text{Cl})\text{n}$  will occur when bombarding a  $^2\text{H}$  target with 2.2 MeV·A  $^{36}\text{S}$ . Other reaction channels are possible, but can be neglected at small beam energies. The two main channels cannot be distinguished unless the  $Q$ -values are very different (as is the case for exotic beams, but not for the present experiment), the proton is detected, or the level scheme of one of the two transfer products is already known. With a neutron separation energy of 1.67 MeV and a proton separation energy of 16.9 MeV  $^9\text{Be}$  can also be considered to be a perfect neutron target. In contrast to deuterium, where in the present case the proton and neutron pickup can occur with equal cross-sections, the proton pickup is strongly suppressed for the beryllium target. Yet, there exist several other reaction channels, where many nucleons are transferred from  $^9\text{Be}$  to the projectile (see sect. 5.3).

The reaction kinematics of both target nuclei are displayed in fig. 1 for the population of the  $3/2_1^-$ -level at 646 keV and the  $1/2_1^-$ -level at 2.64 MeV in  $^{37}\text{S}$ .

The figure shows that in the  $^2\text{H}(^{36}\text{S},^{37}\text{S}^*)\text{p}$  reaction the  $^{37}\text{S}$  nucleus is always deflected by less than  $2.5^\circ$  and travels at about beam velocity regardless of the deflection

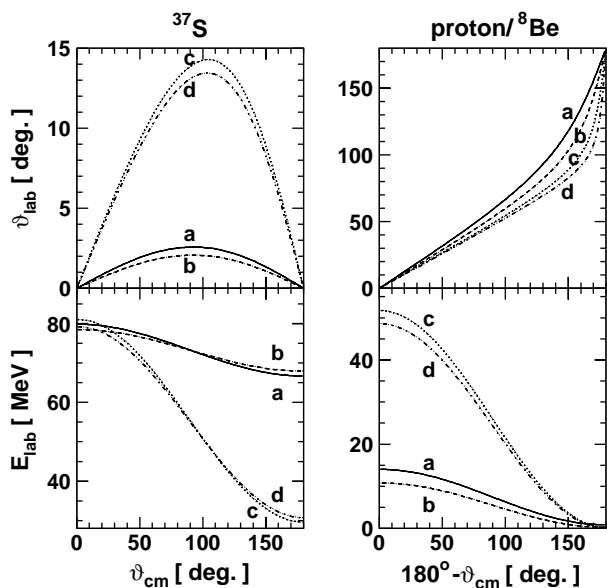


**Fig. 1.** Kinematics of the  ${}^2\text{H}({}^{36}\text{S}, {}^{37}\text{S}^*)\text{p}$  (a,b) and  ${}^9\text{Be}({}^{36}\text{S}, {}^{37}\text{S}^*){}^8\text{Be}$  (c,d) reaction populating the  $3/2^-$  level at 646 keV (a,c) and the  $1/2^-$  level in  ${}^{37}\text{S}$  at 2.64 MeV (b,d). Here  $\vartheta_{\text{cm}}$  is the scattering angle of  ${}^{37}\text{S}$  in the c.m. system, while  $\vartheta_{\text{lab}}$  denotes the laboratory angle and  $E_{\text{lab}}$  the laboratory energy of one of the two reaction products. All angles are measured with respect to the beam axis.

angle. In contrast, the kinematics of the reaction with the beryllium target shows a significantly larger deflection of  ${}^{37}\text{S}$  of up to  $14^\circ$  and a considerable energy variation. Hence one can expect to achieve a sufficient Doppler correction when using a deuterium target even without detecting one of the scattered reaction products, while at least a partial kinematic reconstruction is necessary to calculate the Doppler shift when a beryllium target is used.

From conservation of energy and momentum one finds that for a  $Q$ -value of

$$Q > E_{\text{beam}} \left( \frac{M_{\text{p}}}{M_{\text{pt}}} - 1 \right) \quad (1)$$

the light reaction product can be emitted in backward direction. Here  $E_{\text{beam}}$  is the energy of the beam particles and  $M_{\text{p}}/M_{\text{pt}}$  is the ratio of the projectile masses before and after transfer. For the  ${}^2\text{H}({}^{36}\text{S}, {}^{37}\text{S}^*)\text{p}$  reaction, this condition is fulfilled for excited states up to an energy of 4.23 MeV, as the reaction has a ground state  $Q$ -value of +2.08 MeV. For the  ${}^9\text{Be}({}^{36}\text{S}, {}^{37}\text{S}^*){}^8\text{Be}$  reaction the condition is fulfilled for states up to 4.79 MeV, as the corresponding ground state  $Q$ -value is +2.64 MeV. Thus for both reactions and both excited states in  ${}^{37}\text{S}$  considered, the emission of the light reaction product in backward direction is possible, although its energy will be rather small.

In the proposed transfer experiments the total cross-sections to excited  $\gamma$ -decaying states can be deduced from the  $\gamma$  lines integrated over the full solid angle covered by MINIBALL. However, in order to determine the differential c.m. cross-sections (see fig. 2) one has to trace one of the reaction products. If the variation of the laboratory

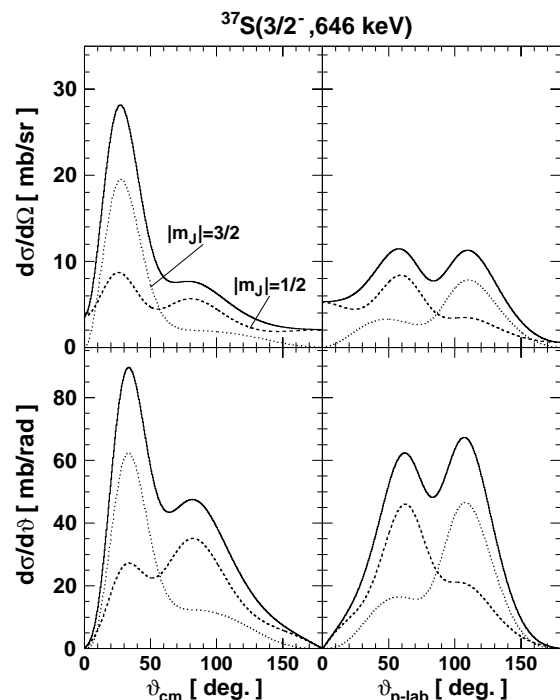


**Fig. 2.** Calculated differential cross-sections for individual  $m$ -substates (dotted and dashed lines) and summed over the  $m$ -substates (solid line) of the  $3/2^-$  level in  ${}^{37}\text{S}$  for the  ${}^2\text{H}({}^{36}\text{S}, {}^{37}\text{S}^*)\text{p}$  reaction at a beam energy of 2.2 MeV·A. Left panels: differential cross-sections in the c.m. system (with  $\vartheta$  denoting the c.m. angle of  ${}^{37}\text{S}$ ). Right panels: differential cross-sections in the laboratory system when detecting the residual proton.

angle and laboratory energy of the excited transfer product with  $\vartheta_{\text{cm}}$  is sufficiently large, this can be achieved by detecting its flight direction and using the Doppler shift to distinguish between forward and backward scattering in the c.m. system. An elegant alternative method is to analyze the Doppler broadened  $\gamma$  lineshapes observed around  $0^\circ$  or  $180^\circ$  with respect to the beam axis, which provide a direct measure of the c.m. cross-section modified by the particle- $\gamma$ -correlation function [10]. Both methods cannot be applied when using a  ${}^2\text{H}$  target. Here it is only feasible to deduce information on the differential cross-sections by measuring at least the direction of the light reaction product together with the decay  $\gamma$ -rays.

While the particle angular dependence of the differential transfer cross-section allows to determine the angular momentum of the transferred nucleon, the total spin of the final states can be deduced from the  $\gamma$ -angular distributions. If necessary one can enhance the anisotropy of the  $\gamma$  distribution by requiring coincidences, *e.g.*, with all forward scattered particles.

### 3 Setup of the experiment

The overall setup of the test experiment is shown in fig. 3. Two six-fold segmented MINIBALL germanium modules

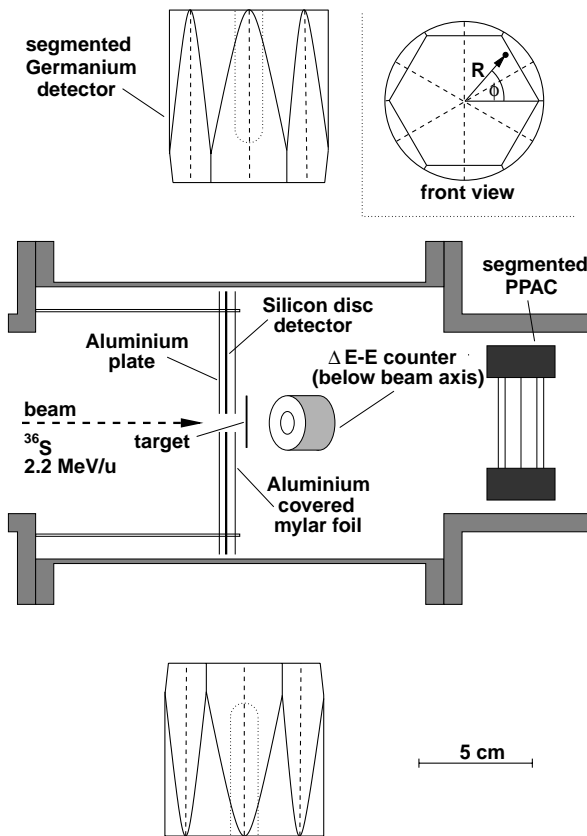


**Fig. 3.** Experimental setup. The tube-shaped target box is shown as cut in half. All detectors are seen from above. The electric segmentation of the germanium detectors is indicated by dashed lines. Detectors and target box are shown in correct proportions. A front view of the germanium detector is shown in the inset and displays the definition of the radius  $R$  and angle  $\phi$  of the  $\gamma$ -ray interaction point.

were used<sup>1</sup> and placed at an angle of  $\vartheta_{\text{det}} = 90^\circ$  with respect to the beam axis at a target distance of 10.6 cm, which is the minimum distance achievable with MINIBALL at REX-ISOLDE. It should be noted that not only the small detector-target distance but also the  $90^\circ$  detection angle correspond to the most demanding conditions with regard to the Doppler shift correction of the recorded  $\gamma$  lines, as for this position the resulting  $\gamma$  line width is most sensitive to the finite granularity of the  $\gamma$  detector.

The detector modules were equipped with preamplifiers for the six segment signals and the core contact. The pulse heights of the charge signal at the core preamplifier was used to obtain the  $\gamma$ -ray energy using standard electronics and a peak-sensing ADC. The energy information of the segments was obtained in the same way and used to deduce an information about the  $\phi$ -angle of the  $\gamma$ -ray entry point (see inset in fig. 3). Besides the energy information of the core and the segments, the differentiated<sup>2</sup>

<sup>1</sup> For the measurement with the deuteron target only one module was available.

<sup>2</sup> A timing filter amplifier was used for differentiation.

preamplifier pulse of the core contact was recorded using a 250 MHz 8-bit Flash-ADC and used to determine the radius  $R$  of the  $\gamma$ -ray entry point [11] as defined in the inset in fig. 3.

The REX-ISOLDE PPAC was positioned at zero degrees with the entry foil 11 cm behind the target. The scattering angles covered by the PPAC reached up to  $\vartheta = 9^\circ$ , so that all heavy reaction products of the  ${}^2\text{H}({}^{36}\text{S}, {}^{37}\text{S})\text{p}$  reaction passed through the detector as  $\vartheta_{37\text{S}} < 2.5^\circ$  (see fig. 1). In order to avoid damage to the PPAC, a mechanical shutter could be inserted in front of the PPAC when the beam intensities exceeded the maximum allowed values of about  $5 \cdot 10^7$  particles/s.

The PPAC consisted of 5 metallized foils and was operated with isopropane gas at a pressure of 5 mbar. The areal density ( $< 1.5 \text{ mg/cm}^2$ ) was sufficiently low to allow particles to traverse the detector without stopping, so that the  $\beta$  background and the  $\gamma$  background from  $\beta$  decay was kept as low as possible. At low beam intensities of up to around  $10^6$  particles/s it was possible to count individual beam particles. At higher particle rates the detector could still be used as a position-sensitive current monitor. A more detailed description of this counter can be found in [9].

In the single-particle readout mode an efficiency of  $>99\%$  was measured with  $\alpha$ -particles (1.4 MeV $\cdot$ A) from an  ${}^{241}\text{Am}$  source at a particle rate of  $10^3 \text{ s}^{-1}$ . In the in-beam experiment a decline of the efficiency was observed for very high rates. At a particle rate of  $10^6$  particles/s an efficiency of 70% (mainly due to deadtime problems) was found. This efficiency was estimated by comparing the peak area of the 646 keV  $\gamma$  line from the decay of  ${}^{37}\text{S}$  produced in the  ${}^2\text{H}({}^{36}\text{S}, {}^{37}\text{S}^*)\text{p}$  reaction in a spectrum taken in coincidence with the PPAC to a spectrum taken without this coincidence. The efficiency decreased to 50% at a rate of  $1.5 \cdot 10^6$  particles/s, while the saturation rate was  $3 \cdot 10^6$  particles/s.

In addition to the PPAC, two auxiliary silicon particle detectors were employed. A silicon ring detector with a thickness of 2 mm was placed at a distance of 12 mm from the target covering backward angles from  $\vartheta = 120^\circ$  to  $\vartheta = 150^\circ$ . The detector was used to investigate the feasibility of observing the light reaction products at backward directions. Although it was possible to trace protons in backward direction, the low particle energies and the noise fluctuations of the silicon detector did not permit a quantitative measurement of backscattered protons in this experiment.

In forward direction a small  $\Delta E$ - $E$  Si-detector-telescope with an active area of  $50 \text{ mm}^2$  and thicknesses of  $50 \mu\text{m}$  and  $1500 \mu\text{m}$ , respectively, was located at a distance of 30 mm from the target at an angle of  $\vartheta = 40^\circ$  with respect to the beam axis. The main application of this detector was the selection of reaction channels by identifying one of the light reaction products. In the REX-ISOLDE setup this small telescope will be replaced by a large position-sensitive annular silicon disc-telescope detector [12]. Both silicon detectors were covered with aluminumized mylar foils with a thickness of  $0.2 \text{ mg/cm}^2$ .

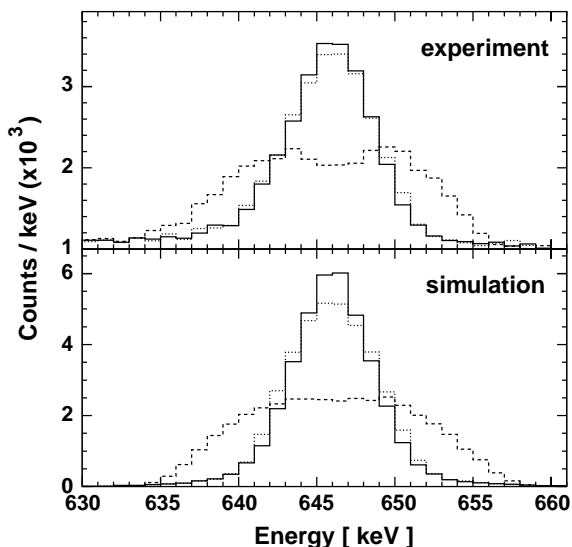


**Fig. 4.** Measured and simulated Doppler-corrected  $\gamma$  line-shapes for the 646.2 keV transition in  $^{37}\text{S}$  produced in the inverse reaction  $^2\text{H}(^{36}\text{S},^{37}\text{S})\text{p}$ . The MINIBALL detector module was placed at  $\vartheta_{\text{det}} = 90^\circ$  at a distance of 10.6 cm. (Dashed line: no entry point information used; dotted line: Doppler-corrected  $\gamma$  line using the segment information; solid line: Doppler-corrected  $\gamma$  line using both segment and radius information.)

A  $^{36}\text{S}^{8+}$  beam with an energy of 79.2 MeV (2.2 MeV $\cdot$ A) was provided from the MPI-K tandem accelerator. The beam was pulsed with a frequency of 13.56 MHz (74 ns) and a pulse width of  $\sim 1$  ns. The beam intensity was varied between  $2 \cdot 10^5$  and  $6 \cdot 10^8$  particles per second. Self-supporting targets of deuterium-enriched polythene ( $\sim 99\%$   $\text{CD}_2$ ,  $\sim 0.5$  mg/cm $^2$ ) and  $^9\text{Be}$  (0.54 mg/cm $^2$ ) were used.

## 4 Feasibility studies

### 4.1 Doppler correction

In MINIBALL the  $\gamma$  detectors will be positioned close to the target to optimize the  $\gamma$ -detection efficiency. As the recoil velocities encountered in inverse reactions are large, the Doppler broadening of the  $\gamma$  lines, due to the large solid angle covered by a single detector module, will therefore be severe.

In order to examine the capabilities offered by the segmented germanium detectors in improving the  $\gamma$  line widths, the 646.2 keV line from the decay of the first excited state of  $^{37}\text{S}$  populated in the  $^2\text{H}(^{36}\text{S},^{37}\text{S}^*)\text{p}$  reaction at a beam energy of 2.2 MeV $\cdot$ A was investigated in more detail. In the Doppler shift analysis, the flight direction of  $^{37}\text{S}$  was assumed to be given by the beam axis and its average recoil velocity was taken to be  $\beta = 6.5\%$  of the velocity of light, thereby accounting for the energy loss of the S ions of 10% in the target.

Without any additional information on the entry point of the  $\gamma$ -ray into the detector an energy resolution of only

13.6 keV can be obtained for the 646.2 keV  $^{37}\text{S}$  line as compared to the intrinsic resolution of 1.7 keV (see upper panel in fig. 4). Applying the  $\phi$ -angle algorithm (assuming an average  $\gamma$ -ray entry radius of  $R = 20$  mm) the  $\gamma$  line width is reduced by a factor of 2 to 6.7 keV. The angle algorithm only relies on the segment energy information and is based on the fact that the first interaction point of the  $\gamma$ -ray in the detector material, which carries the directional information, and the main interaction of the  $\gamma$ -ray, where the maximum energy is deposited, are usually located close together in the  $(R, \phi)$  space (see inset in fig. 3). A full description of the algorithms used can be found in [4]. If the additional radius information—derived from the differentiated core pulse shape data with a resolution of  $\pm 5$  mm by applying the steepest-slope algorithm [11]—is included in the Doppler correction, the  $\gamma$  line width can be further decreased to 6.2 keV. The GEANT simulations shown in the lower panel of fig. 4 give similar results (13.5 keV, 6.3 keV, and 5.6 keV, respectively). The small differences between the simulation and the measurement remaining after considering also the intrinsic resolution of 1.7 keV are due to the angle variation of the recoiling  $^{37}\text{S}$  nuclei of up to  $\pm 2.5^\circ$ , which was disregarded in the simulation.

The final MINIBALL electronics will also support a detailed pulse shape analysis of the segment signals. This allows for a more precise determination of the position of the main interaction point of the  $\gamma$ -ray and therefore for a further improvement of the Doppler corrected  $\gamma$  line width [4,5]. Indeed, recent measurements with collimated  $\gamma$  sources have shown that a granularity of almost 100 can be reached for the solid angle subtended by a MINIBALL module when the full pulse shape analysis offered by the new MINIBALL electronics is employed. For the special case considered here ( $\vartheta_{\text{det}} = 90^\circ$ ,  $\beta = 0.065$ ,  $E_\gamma = 646$  keV) and neglecting the intrinsic detector resolution of 1.7 keV, we expect according to our simulations, an energy resolution after Doppler correction of 3.6 keV if the flight direction of the  $\gamma$ -emitting  $^{37}\text{S}$  nucleus is assumed to be exactly known ( $0^\circ$ ). A value of 4.7 keV is obtained when averaging over the recoil angles of the  $^{37}\text{S}$  nuclei. It should be noted again that the special case considered here corresponds to the most demanding setup of a MINIBALL module with regard to the Doppler correction. Considerably smaller line widths can be expected for all those modules of the MINIBALL array positioned at angles  $\vartheta_{\text{det}} \neq 90^\circ$ .

### 4.2 Background reduction

The background suppression achieved with the REX-ISOLDE PPAC was investigated using the  $^2\text{H}(^{36}\text{S},^{37}\text{S}^*)\text{p}$  reaction at low beam intensities of  $10^6$  particles/s. The results are displayed in fig. 5. In the raw germanium spectrum, shown in panel (a), the 646 keV de-excitation  $\gamma$  line of the first excited state in  $^{37}\text{S}$  is hardly visible between the narrow background peaks. When the Doppler correction is applied (panel (b)) the 646 keV line becomes more pronounced as its width is reduced, while the background

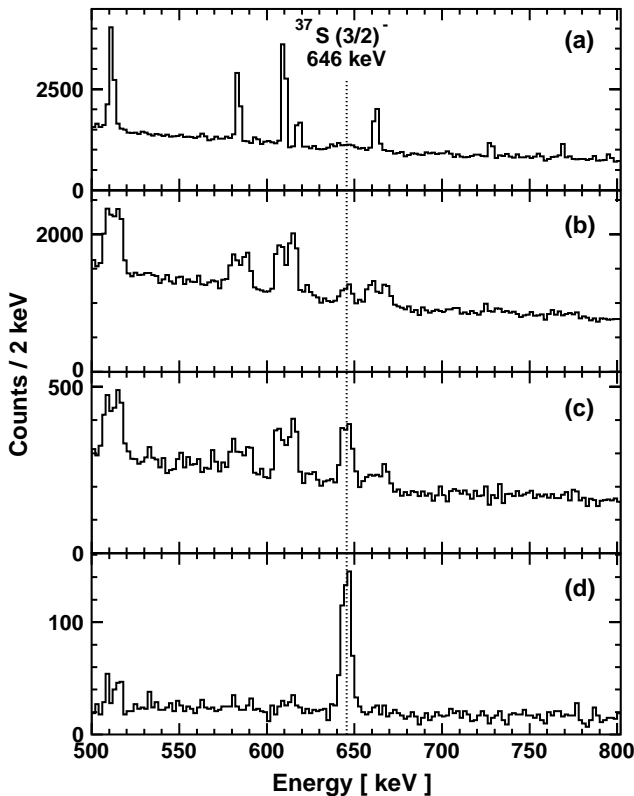


**Fig. 5.** Partial  $\gamma$ -ray spectra following the  $^{36}\text{S} \rightarrow ^2\text{H}$  reaction. The events were measured with one of the germanium modules in a beam time of 7 hours at a beam intensity of  $10^6$  particles/s. In the panels is shown: (a) the raw  $\gamma$  single spectrum; (b) the same as in panel (a), but with the Doppler correction relevant for the neutron pickup reaction applied; (c) the same as (b), but a coincidence of the  $\gamma$  signal with the accelerator RF was required; (d) the same as (c), but an additional coincidence with the PPAC signal was required, resulting in an essentially background free spectrum.

lines are broadened. The de-excitation line is now visible on top of the background with a peak-to-background ratio of 10%. Requiring a coincidence of the germanium signal with the RF signal, controlling the beam pulsing system of the accelerator, the background is reduced by more than a factor of 5 (panel (c)) as the Ge-detector is no longer active in between the beam pulses. The peak areas of the 646 keV line in both spectra agree within statistical limits, *i.e.* the detector efficiency is not reduced by the coincidence requirement.

An almost background-free  $\gamma$ -spectrum is obtained when an additional coincidence with the PPAC is required (panel (d)). Although the peak area of the 646 keV line is suffering a loss of about 30% due to the reduced efficiency of the PPAC at particle rates of  $10^6$  particles/s, the background is reduced by another factor of  $\sim 13$ . This reduction is caused by the fact that for a beam-pulse frequency of 13.56 MHz and a beam intensity of  $10^6$  particles/s, on the average only every 14th beam pulse contains a projectile. Thus by requiring the PPAC coincidence, background  $\gamma$ -rays accumulated when an empty beam bunch arrives

are rejected. Note that no background spectra have been subtracted from the spectra shown in fig. 5. By doing so, the small remaining background in fig. 5d can be quantitatively removed.

In the present experiment the incoming beam consisted of the stable  $^{36}\text{S}$  nucleus. In an experiment with  $\beta$ -unstable beam nuclei the background situation will be more severe, due to the  $\beta$ -decay of radioactive nuclei scattered on the target. However, in the transfer reactions studied here most beam particles will pass through the PPAC and will be caught by the beam dump, which is well shielded towards the detector array. Only the small fraction of the incoming beam particles that scatter on the carbon nuclei, also present in the  $\text{CD}_2$  target, to angles larger than  $9^\circ$  will be dumped in the target chamber. When heavier target nuclei are used (*e.g.*, for Coulomb excitation) the background will be substantially higher; however, it will not reach prohibitively high levels as demonstrated in [6].

## 5 Results

### 5.1 Reaction channels on the $\text{CD}_2$ target

Bombarding a deuterium target with beams having an energy of  $2.2 \text{ MeV} \cdot \text{A}$   $^{36}\text{S}$ , the two strongest reaction channels will be the neutron and the proton pickup. As REX-ISOLDE is designed to explore new regions of unknown nuclei, this is an important advantage, as for the assignment of the observed  $\gamma$  transitions only two possible nuclei have to be considered. Furthermore, the resulting transfer nuclei travel at about the same speed and in the same direction as the beam particles allowing a Doppler correction of the  $\gamma$  lines without the need to determine the kinematics by particle detection. However, pure deuterium targets are not readily available. Thus deuterium-enriched polythene  $(\text{CD}_2)_n$  is widely used as a target material. Polythene is easy to handle and foils of any desired thickness can be produced. However, additional reaction channels may occur due to the presence of the carbon.

In fig. 6 the Doppler-corrected  $\gamma$  spectrum observed at  $\vartheta_{\text{det}} = 90^\circ$  in coincidence with the PPAC and the accelerator RF when bombarding a  $(\text{CD}_2)_n$  target with a  $^{36}\text{S}$  beam is displayed. The spectrum was recorded in 24 hours at a beam intensity of  $1 \cdot 10^6$  particles/s and a beam energy of  $2.2 \text{ MeV} \cdot \text{A}$ . The Doppler correction was performed as discussed in section 4.1.

Prominent lines from the de-excitation of the neutron pickup product  $^{37}\text{S}$  occur at 646 keV, 1347 keV, and 1993 keV. At 1727 keV and at 3117 keV  $\gamma$  lines from the proton pickup product  $^{37}\text{Cl}$  are observed, the latter line being composed of two known  $^{37}\text{Cl}$  lines at 3086 keV and 3103 keV. The lines at 890 keV, 1122 keV, and 1289 keV are due to  $\gamma$ -transitions in  $^{46}\text{Ti}$  populated in the fusion-evaporation reaction  $^{12}\text{C}(^{36}\text{S}, 2n)^{46}\text{Ti}$ . A list of all strong  $\gamma$  transitions observed, their assignment, and their relative  $\gamma$  intensities is given in table 1.

In the reaction investigated in this test experiment all reaction products are well known; however, when

**Table 1.** Compilation of the strongest  $\gamma$  lines observed at  $\vartheta_{\text{det}} = 90^\circ$  in the reaction  $^{36}\text{S} \rightarrow \text{CD}_2$  at an energy of 2.2 MeV·A. In the different columns are listed, respectively, the transition energies extracted from Doppler-corrected spectra using the reaction-specific kinematics; literature values are given in italics; the number of  $\gamma$ -rays observed in a high statistics run performed without PPAC coincidences; the deduced transition, based on the level energy:  $^{37}\text{S}$ :  $^2\text{H}(^{36}\text{S}, ^{37}\text{S}^*)\text{p}$ ,  $^{37}\text{Cl}$ :  $^2\text{H}(^{36}\text{S}, ^{37}\text{Cl}^*)\text{n}$ ,  $^{46}\text{Ti}$ :  $^{12}\text{C}(^{36}\text{S}, ^{46}\text{Ti}^*2\text{n})$ ; the relative cross-sections assuming isotropic emission of the  $\gamma$ -rays; the absolute cross-sections (see text).

$E_\gamma$ (keV)	$N_\gamma$	reaction & transition	$\frac{\sigma_\gamma(E)}{\sigma_\gamma(646)}$	$\sigma_\gamma(E_\gamma)$ (mb)
646(1) ( <i>646</i> )	19500 (5%)	$^{37}\text{S}$ : $3/2_1^- \rightarrow 7/2_{\text{gs}}^-$	100%	215(43)
— ( <i>751</i> )	<500	$^{37}\text{S}$ : $3/2_1^+ \rightarrow 3/2_1^-$	<3%	<5
1347(3) ( <i>1346</i> )	1000 (40%)	$^{37}\text{S}$ : $3/2_2^- \rightarrow 3/2_1^-$	8%	19(10)
— ( <i>1377</i> )	<400	$^{37}\text{S}$ : $7/2_1^- \rightarrow 3/2_1^-$	<3%	<5
1993(2)* { ( <i>1992</i> )	3100 (10%)	$^{37}\text{S}$ : $3/2_2^- \rightarrow 7/2_{\text{gs}}^-$	29%	61(14)
( <i>1992</i> )		$^{37}\text{S}$ : $1/2_1^- \rightarrow 3/2_1^-$		
— ( <i>2023</i> )	<300	$^{37}\text{S}$ : $7/2_1^- \rightarrow 7/2_{\text{gs}}^-$	<3%	<5
1727(3) ( <i>1727</i> )	1800 (20%)	$^{37}\text{Cl}$ : $1/2_1^+ \rightarrow 3/2_{\text{gs}}^+$	16%	33(10)
3101(5)* { ( <i>3086</i> )	3200 (10%)	$^{37}\text{Cl}$ : $5/2_1^+ \rightarrow 3/2_{\text{gs}}^+$	45%	98(23)
		$^{37}\text{Cl}$ : $7/2_1^- \rightarrow 3/2_{\text{gs}}^+$		
3748(10) ( <i>3741</i> )	300 (50%)	$^{37}\text{Cl}$ : $5/2_1^- \rightarrow 3/2_{\text{gs}}^+$	5%	9(5)
890(1) ( <i>889</i> )	6800 (8%)	$^{46}\text{Ti}$ : $2_1^+ \rightarrow 0_{\text{gs}}^+$	85%	187(42)
1049(3) ( <i>1049</i> )	800 (40%)	$^{46}\text{Ti}$ : $3_1^- \rightarrow 4_1^+$	11%	23(9)
1122(1) ( <i>1121</i> )	5500 (10%)	$^{46}\text{Ti}$ : $4_1^+ \rightarrow 2_1^+$	77%	168(37)
1289(2) ( <i>1289</i> )	1900 (20%)	$^{46}\text{Ti}$ : $6_1^+ \rightarrow 4_1^+$	28%	61(19)

\* The two transitions could not be resolved.

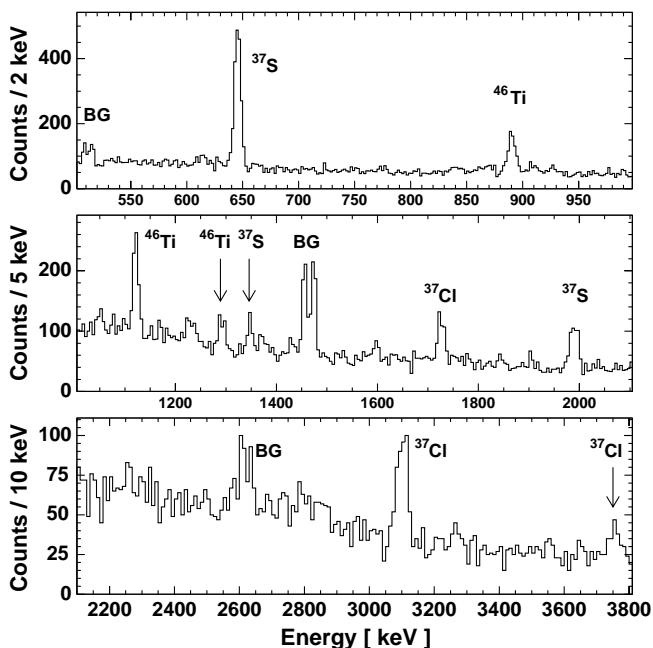


**Fig. 6.** Doppler-corrected PPAC-gated germanium spectrum without background subtraction observed in the  $^{36}\text{S} \rightarrow (\text{CD}_2)_n$  reaction at 2.2 MeV·A. The spectrum was taken in a 24 hours beamtime at a beam intensity of  $1 \cdot 10^6$  particles/s with a single germanium detector at  $\vartheta_{\text{det}} = 90^\circ$ . The spectrum corresponds to that of fig. 5d, but here the full energy range and the full statistics are also shown.

exploring unknown regions of the nuclear chart it is necessary to distinguish the  $\gamma$ -transitions emitted from

the transfer products from background and  $\gamma$ -transitions caused by other reaction channels.

Background  $\gamma$  lines are easily recognized as these lines become broader after the Doppler correction. Thus they can be immediately identified and eliminated by background subtraction. The background spectrum can be obtained by recording a  $\gamma$  single spectrum in anti-coincidence with the accelerator RF and the PPAC.

The different Doppler shifts of  $\gamma$  lines emitted from transfer and fusion products can also be used to distinguish between these two channels. When  $\gamma$  lines produced in fusion reactions are Doppler corrected with the transfer kinematics the resulting peak position will still depend on the  $\gamma$ -observation direction. As a result, the fusion lines in the Doppler-corrected sum spectra obtained, *e.g.*, by summing over all MINIBALL modules in the forward and in the backward direction separately will be broadened and centered at different energies.

It is more demanding to separate the two pickup channels since, unless the  $Q$ -values are very different (as is the case for exotic nuclei, but not here), they show the same kinematics and Doppler behavior. If a  $\gamma$ -transition is already known in one of the nuclei  $\gamma$ - $\gamma$  coincidences may help to identify further transitions. Otherwise, one can either use the large annular silicon detector available in REX-ISOLDE experiments in the forward hemisphere to detect the proton leftover in the neutron pickup reaction, or perform the same measurement with the  $^9\text{Be}$  target, where the proton pickup is suppressed (see sect. 5.3).

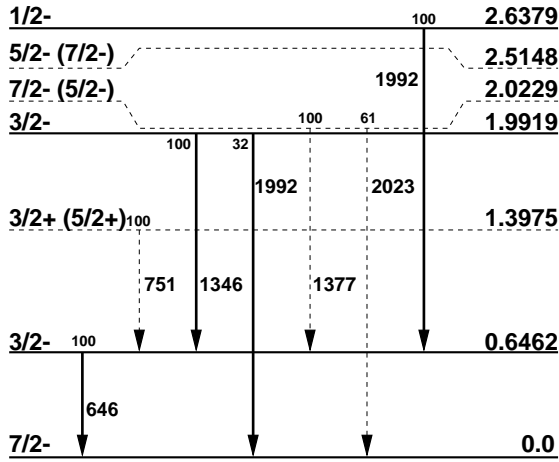


**Fig. 7.** Level scheme of  $^{37}\text{S}$ . The  $\gamma$  transitions observed are marked by thick arrows, levels populated are shown with bold lines. Level energies and branching ratios are taken from [13].

## 5.2 Cross-section determination for the $\text{CD}_2$ target

The experimental setup allows to determine absolute cross-sections rather easily, since the total number of beam particles which have passed the target during beamtime is available from the REX-ISOLDE PPAC. Together with the number of counts in a  $\gamma$  line at energy  $E_\gamma$  (deduced from the  $\gamma$  spectrum observed in coincidence with the PPAC), the known areal density of the deuterium in the  $\text{CD}_2$  target, and the efficiency of the germanium detectors  $\varepsilon_{\text{Ge}}(E_\gamma)$  it is possible to derive the absolute cross-sections  $\sigma_\gamma(E_\gamma)$  for the  $\gamma$  line by

$$\begin{aligned} \sigma_\gamma(E_\gamma) &= \frac{N_{\gamma\text{-PPAC}}(E_\gamma) / (\varepsilon_{\text{Ge}}(E_\gamma) \cdot \varepsilon_{\text{PPAC}})}{p \cdot (N_{\text{PPAC}} / \varepsilon_{\text{PPAC}}) \cdot (N/A)_{\text{deuteron}}} \\ &= \frac{N_{\gamma\text{-PPAC}}(E_\gamma) / \varepsilon_{\text{Ge}}(E_\gamma)}{p \cdot N_{\text{PPAC}} \cdot (N/A)_{\text{deuteron}}} \end{aligned} \quad (2)$$

Here  $N_{\gamma\text{-PPAC}}(E_\gamma)$  is the number of  $\gamma$ -rays, which were observed in the germanium detector in coincidence with the PPAC,  $\varepsilon_{\text{Ge}}(E_\gamma)$  the energy-dependent full-energy peak efficiency of the germanium detector,  $\varepsilon_{\text{PPAC}}$  the detection efficiency of the PPAC,  $N_{\text{PPAC}}$  the number of beam particles counted by the PPAC, and  $(N/A)_{\text{deuteron}}$  denotes the deuteron areal density in the target given in atoms/cm<sup>2</sup>. The areal density of the  $\text{CD}_2$  target of 0.55 mg/cm<sup>2</sup>, used in the present experiment, corresponds to  $(N/A)_{\text{deuteron}} = 4.1 \cdot 10^{19} \text{ cm}^{-2}$  and  $(N/A)_{^{12}\text{C}} = 2.1 \cdot 10^{19} \text{ cm}^{-2}$ . The factor  $p$  takes into account that due to the time structure of the beam (1 ns wide pulses every 74 ns) there exist a non-zero probability that more than one projectile is contained in one beam pulse, which cannot be distinguished by the Ge-RF-PPAC coincidence requirement. In the present experiment  $p$  is approximately given by  $p = 1.07(2)$ .

It is important to note that the efficiency of the PPAC cancels out so that this method allows to derive absolute cross-sections without the knowledge of the efficiency of the PPAC. One should also be aware that in equation (2) a possible angular distribution of the emitted  $\gamma$ -rays with

$E_{\text{level}}$ (keV)	$J^\pi$	$\sigma_{\text{exp.}}$ (mb)	$\sigma_{\text{theo.1}}$ (mb)	$\sigma_{\text{theo.2}}$ (mb)
646	$3/2^-$	140(46)	180	105
1992	$3/2^-$	23(10)	-	-
2638	$1/2^-$	56(15)	95	75

**Table 2.** Comparison of the experimental and calculated total cross-sections for three excited states in  $^{37}\text{S}$  populated in  $^2\text{H}(^{36}\text{S}, ^{37}\text{S}^*)\text{p}$  neutron pickup reaction at 2.2 MeV·A.

respect to the beam direction is neglected; the formula is exact for isotropic  $\gamma$ -ray emission, otherwise a correction factor is needed. However, this factor reduces to 1 if the full MINIBALL array is used as the array covers all regions of the full  $4\pi$  solid angle equally well.

Using equation (2) and the intensity data accumulated in the 24 hour beamtime at a beam intensity of  $10^6$  particles/s, an absolute cross-section of 215(43) mb has been derived for the 646 keV  $\gamma$  line of  $^{37}\text{S}$  assuming an isotropic  $\gamma$ -angular distribution (see further below). The uncertainty of the cross-section value comprises statistical errors, the error of the target thickness (5%), and the uncertainty in the efficiency of the germanium detector (15%).

With the absolute cross-section for the 646 keV line the cross-sections can be deduced for other  $\gamma$  lines from the relative  $\gamma$  intensities, which were deduced in the present case from a high statistic run without requiring PPAC-coincidences (see table 1).

While the cross-sections  $\sigma_\gamma(E_\gamma)$  for the occurrence of a  $\gamma$ -ray of energy  $E_\gamma$  are directly accessible, the relevant spectroscopic data is the cross-section  $\sigma(E)$  to directly populate a certain excited level of energy  $E$ . Both kinds of cross-sections are linked by the branching ratios for the different de-excitation channels. While the branching ratios for the decay of excited states of  $^{37}\text{S}$  populated in this experiment are already known [13], information about the level scheme and the branching ratios of unknown nuclei investigated in REX-ISOLDE experiments will have to be extracted from the measurement.

With the aid of the level scheme of  $^{37}\text{S}$  and the branching ratios (see fig. 7) the cross-section  $\sigma(E)$  was calculated. The population of three negative-parity low spin levels was observed: the absolute cross-section for the population of the  $3/2_1^-$ -level at 646 keV, the  $3/2_2^-$ -level at 1992 keV, and the  $1/2_1^-$  level at 2638 keV was 140(46) mb, 23(10) mb, and 56(15) mb, respectively (see table 2). The two states which were most strongly populated correspond to the  $^{36}\text{S}$  core and an excited neutron in the  $2p_{3/2}$  ( $3/2_1^-$ ) and  $2p_{1/2}$  ( $1/2_1^-$ ) shell. A simple classical estimate, which assumes a  $^{36}\text{S}$ -nucleus, a single neutron, and a relative velocity corresponding to an energy of 2.2 MeV·A, shows that the most probable angular momentum transfer is  $1\hbar$ . Hence, transfer to excited states with high orbital angular momenta are expected to be suppressed; as a consequence the population of the  $1f_{5/2}$  and  $1f_{7/2}$  single neutron states was not observed.



The  $^{36}\text{S}(d,p)^{37}\text{S}$  reaction was studied before using an accelerated deuteron beam. The beam energy in these cases was between 10 MeV and 20 MeV and the obtained cross-sections can therefore not be compared to this experiment. L.M. Solin *et al.* reported in [14] a measurement using a deuteron beam with an energy of 3.55 MeV, but no cross-sections were reported.

The here measured cross-sections were compared with theoretical predictions (listed in table 2). Skyrme-Hartree-Fock calculations were used to derive the structure of the nuclei. The results were used to obtain transfer probabilities using the Distorted-Wave-Born-Approximation (DWBA) and the Exact-Finite-Range-Distorted-Wave-Born-Approximation (EFR-DWBA) (for details see [8]). When the level energies obtained in the theoretical calculations were used, theoretical model cross-sections of  $\sigma(3/2_1^-) = 180$  mb and  $\sigma(1/2^-) = 95$  mb were derived, whereas cross-sections of  $\sigma(3/2_1^-) = 105$  mb and  $\sigma(1/2^-) = 75$  mb were found when the level energies were fixed at their experimental values. The agreement of the latter results with the experimental values is fair.

For the calculations of the experimental cross-sections isotropic angular distributions of the  $\gamma$ -rays emitted from the excited nuclei were assumed. While this assumption is always true for  $J = 1/2$  states, it applies for the  $3/2$  levels only, if all  $m$ -substates are populated equally. Although the differential cross-sections to populate the  $|m| = 1/2$  and the  $|m| = 3/2$  substates of the  $3/2_1^-$  level differ significantly, as can be seen in fig. 2, the angle-integrated total probabilities to populate these substates are 48% and 52%, respectively, and the angular distribution of the emitted  $\gamma$ -rays deviates by less than 1% from an isotropic distribution. Even if one assumed complete alignment, the deviation would be less than 14%.

In the anticipated REX-ISOLDE experiments the full MINIBALL will be used, which subtends the  $4\pi$  solid angle of the de-excitation  $\gamma$ -rays rather isotropically. This will facilitate the determination of the absolute cross-sections  $\sigma_\gamma(E_\gamma)$ , the branching ratios needed to derive the corresponding total cross-section  $\sigma(E)$  as well as the differential cross-sections  $d\sigma/d\Omega$ . Moreover,  $\gamma$  angular distributions,  $\gamma$ - $\gamma$  and  $\gamma$ -particle correlations are in principle accessible allowing to derive level schemes, spins, and parities. In favorable cases even lifetime measurements will be possible (see, *e.g.*, [15]).

### 5.3 Beryllium-induced transfer

In contrast to the deuterium target the proton pickup is strongly suppressed as compared to the neutron pickup when using the  $^9\text{Be}$  target, thus facilitating the identification of the latter reaction channel. Yet  $^9\text{Be}$  exhibits two significant disadvantages as a target. Besides the neutron pickup reaction  $^9\text{Be}(^{36}\text{S}, ^{37}\text{S}^*)^8\text{Be}$  there exist several fusion-evaporation channels. Furthermore,  $^9\text{Be}$  is significantly heavier than deuterium and the reaction products are deflected by larger angles and are subject to larger energy variations (see fig. 1), and a good Doppler correction can only be achieved by tracking the direction of one of

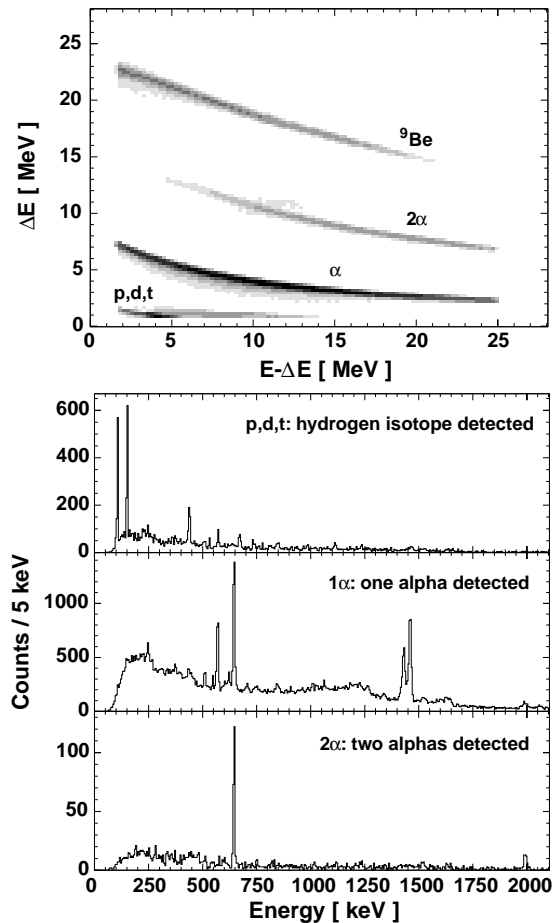


**Fig. 8.** Doppler-corrected  $\gamma$  spectra observed in the  $^{36}\text{S} \rightarrow ^9\text{Be}$  reaction at 2.2 MeV·A are shown in the bottom plot. The spectra were generated by gating on the particle branches identified in the  $\Delta E-(E - \Delta E)$  matrix of the silicon telescope detector (top plot).

the reaction products. For the present test measurement an 8 hour run with a high intensity ( $6 \cdot 10^8$  particles/s)  $^{36}\text{S}$  beam of 2.2 MeV·A was performed, because in the present setup only a small silicon telescope detector was available for this task. Consequently, the REX-ISOLDE PPAC had to be protected against the beam particles with an aluminum shutter.

As manifested in fig. 8, the silicon  $\Delta E-E$  detector is a major aid to distinguish between different reaction channels and to perform the proper Doppler shift correction. Putting a gate on the hydrogen isotopes yielded several  $\gamma$  transitions mainly at low energies, which could be assigned to potassium isotopes corresponding to the  $^9\text{Be}(^{36}\text{S}, p2n)^{42}\text{K}$  and  $^9\text{Be}(^{36}\text{S}, pn)^{43}\text{K}$  reactions (top panel in the bottom plot of fig. 8). Gating on one  $\alpha$ -particle  $\gamma$ -rays of argon isotopes produced in the  $^9\text{Be}(^{36}\text{S}, \alpha 2n)^{39}\text{Ar}$  and the  $^9\text{Be}(^{36}\text{S}, \alpha n)^{40}\text{Ar}$  reaction as well as of  $^{37}\text{S}$  from the neutron pickup reaction are observed. Requiring both  $\alpha$ -particles originating from the  $^8\text{Be}$  decay, the  $^{37}\text{S}$  neutron pickup channel  $^9\text{Be}(^{36}\text{S}, ^{37}\text{S}^*)2\alpha$  can be selected exclusively. The intensity drop of the 646 keV  $^{37}\text{S}$  line when requiring the detec-

tion of both  $\alpha$ -particles as compared to one  $\alpha$ -particle is due to the small solid angle of the telescope detector used. In the REX-ISOLDE setup this efficiency loss will be substantially smaller because of the large solid angle subtended by the annular telescope detector planned to be employed in these measurements. The  $\gamma$  transitions not shown in the gated spectra could be assigned to calcium isotopes from the fusion-evaporation channels  ${}^9\text{Be}({}^{36}\text{S}, 3n){}^{42}\text{Ca}$  and  ${}^9\text{Be}({}^{36}\text{S}, 2n){}^{43}\text{Ca}$ . An overview of the strongest  $\gamma$  transitions detected is given in [4].

It is interesting to note that the  ${}^{43}\text{K}$  line at 738 keV has a long lifetime of 200 ns. As the beam particles travel about 2 cm/ns and the PPAC was covered with an aluminum shutter plate in this measurement, the line is only visible as a sharp peak if no Doppler correction is performed as most nuclei  $\gamma$ -decay after being stopped in the shutter. For REX-ISOLDE the population of excited states with a lifetime of more than a few nanoseconds will pose problems, as the reaction products will not be stopped in the target chamber and their decay  $\gamma$ -rays will therefore remain undetected.

As no low intensity measurements with the PPAC were performed using the beryllium target, absolute cross-sections for the  ${}^9\text{Be}({}^{36}\text{S}, {}^{37}\text{S}^*){}^8\text{Be}$  reaction could not be deduced, but the relative  $\gamma$  intensities for the different nuclei and states populated in the  ${}^{36}\text{S}\rightarrow{}^9\text{Be}$  reaction could be determined. The fusion-evaporation is the strongest channel leading mainly to  ${}^{42}\text{Ca}$  (85%) and  ${}^{43}\text{Ca}$  (40%),  ${}^{42}\text{K}$  (50%) and  ${}^{43}\text{K}$  (25%) as well as  ${}^{40}\text{Ar}$  (100%) and  ${}^{39}\text{Ar}$  (5%). The neutron pickup leading to  ${}^{37}\text{S}$  (100%) served as the reference cross-section. As expected, no  ${}^{37}\text{Cl}$  lines from the proton pickup channel were observed; for the population probability an upper limit of 2% can be given.

## 6 Summary

A test experiment was performed to investigate the feasibility of  $\gamma$ -ray spectroscopy experiments using inverse transfer reaction with low-intensity radioactive beams.

Two single modules of the MINIBALL germanium array were used to detect the de-excitation  $\gamma$ -rays. By exploiting the six-fold segmentation of the detector modules a relative  $\gamma$  energy resolution of  $< 1\%$  could be achieved after the Doppler shift correction, even though the recoil velocities of the  $\gamma$ -emitting nuclei were as large as  $\beta = 0.065$  and the detectors were placed at a distance of only 10.6 cm from the target at the most unfavorable detection angle of  $90^\circ$  with respect to the recoiling nuclei. This is an improvement of the  $\gamma$  line width by more than a factor of 2 as compared to a module without segmentation and when no pulse shape analysis is used. A further improvement of the  $\gamma$  energy resolution by almost another factor of 2 will be possible when the new MINIBALL electronics is available. The new electronics will allow to exploit the signal shapes of the segment pulses (in addition to the core pulses) to further improve the  $\gamma$ -ray entry point determination.

The new REX-ISOLDE PPAC delivered a time reference signal for particle- $\gamma$  coincidence measurements al-

lowing to perform  $\gamma$  spectroscopy at very low rates. The  $\gamma$ -rays detected without a beam particle were rejected, so that the peak-to-background ratio became independent of the beam particle rate. Furthermore, the PPAC allowed to count individual beam particles up to a rate of  $10^6$  particles/s. Hence an easy method to determine absolute cross-sections was available, as the efficiency of the PPAC does not need to be known.

In the  ${}^{36}\text{S}\rightarrow(\text{CD}_2)_n$  reaction three reaction channels were observed. Besides the deuteron-induced neutron and proton transfer channels leading to  ${}^{37}\text{S}$  and  ${}^{37}\text{Cl}$  also the fusion-evaporation channel  ${}^{12}\text{C}({}^{36}\text{S}, 2n){}^{46}\text{Ti}$  is found to contribute to the  $\gamma$  spectrum. Due to the different Doppler shift of the  $\gamma$  lines it is possible to distinguish between fusion and pickup reactions. The additional identification of the neutron pickup channel requires either the coincident detection of the proton or an additional measurement with a  ${}^9\text{Be}$  target.

Model calculations to predict the neutron pickup cross-sections were performed for two states populated in the  ${}^2\text{H}({}^{36}\text{S}, {}^{37}\text{S}^*)\text{p}$  reaction. The results agree reasonably well with the measurements.

The  ${}^9\text{Be}$  target gives complementary information about the neutron pickup reaction. In addition, neutron-rich compound nuclei are populated, which will be of considerable interest as well when using neutron-rich exotic beams. However, it is mandatory in this case to have a position-sensitive silicon telescope available to detect the light reaction products to be able to distinguish between the different reaction channels and to perform the proper Doppler shift correction.

The present experiment has clearly demonstrated that it is possible to investigate exotic nuclei at REX-ISOLDE using pickup reactions and  $\gamma$ -ray spectroscopy. When MINIBALL is fully equipped and a  $\text{CD}_2$  target with an areal density of  $0.5 \text{ mg/cm}^2$  is used, it will take 20 hours to accumulate 400 counts in a  $\gamma$  line at 1 MeV assuming a beam intensity of  $10^4$  particles/s, a cross-section of  $\sigma_\gamma(E_\gamma) = 100 \text{ mb}$  and a MINIBALL efficiency of 14%.

This work was partly supported by the BMBF under contract No. 06DA915I and the DFG under contract No. Le439/4.

## References

1. D. Habs, O. Kester, T. Sieber, A. Kolbe, J. Ott, G. Bollen, F. Ames, D. Schwalm, R. von Hahn, R. Repnow, H. Podlech, A. Schempp, U. Ratzinger, L. Liljeby, K.-G. Rensfelt, F. Wenander, B. Jonsson, G. Nyman, P. Van Duppen, M. Huysse, A. Richter, G. Shrieder, and G. Walter, Nucl. Instrum. Methods Phys. Res. B **139**, 128 (1998).
2. J. Eberth, H.-G. Thomas, D. Weisshaar, F. Becker, B. Fiedler, S. Skoda, P. von Brentano, C. Gund, L. Palafox, P. Reiter, D. Schwalm, D. Habs, T. Servene, R. Schwengner, H. Schnare, W. Schulze, H. Prade, G. Winter, A. Jungclauss, C. Lingk, C. Teich, and K.-P. Lieb, Prog. Part. Nucl. Phys. **38**, 29 (1997).
3. H.G. Thomas, *Entwicklung eines Germanium-CLUSTER Detektors für das Gamma-Spektrometer EUROBALL*, Dissertation, Universität zu Köln, (Verlag Dr. Köster, Berlin, 1995).

4. C. Gund, Dissertation, Universität Heidelberg, 2000.
5. D. Weisshaar, Dissertation, Universität zu Köln, 2001.
6. W.N. Catford, S. Mohammadi, P.H. Regan, C.S. Purry, W. Gelletly, P.M. Walker, G.J. Gyapong, J. Simpson, D.D. Warner, T. Davinson, R. Neal, R.D. Page, A.C. Shotter, I.M. Hibbert, R. Wadsworth, S.A. Forbes, A.M. Bruce, C. Thwaites, P. Thirolf, P. Van Duppen, W. Galster, A. Ninane, J. Vervier, P. Decrock, M. Huyse, J. Szerypo, J. Wauters, Nucl. Instrum. Methods Phys. Res. A **371**, 449 (1996).
7. G. Vancraeynest, C.R. Bain, F. Binon, R. Coszach, T. Davinson, P. Decrock, T. Delbar, P. Duhamel, M. Gaelens, W. Galster, J.-S. Graulich, M. Huyse, P. Leleux, I. Licot, E. Lienard, P. Lipnik, C. Michotte, A. Ninane, R.D. Page, P.J. Sellin, A.C. Shotter, C. Suekoesd, P. van Duppen, J. Vanhorenbeeck, J. Vervier, M. Wiescher, P.J. Woods, Nucl. Phys. A **616**, 107 (1997).
8. H. Lenske and G. Schrieder, Eur. Phys. J. A **2**, 41 (1998).
9. J. Cub, C. Gund, G. Ickert, J. v. Kalben, D. Pansegrau, G. Schrieder, and H. Stelzer, Nucl. Instrum. Methods Phys. Res. A **453**, 522 (2000).
10. D. Pelte and D. Schwalm, in: *Heavy Ion Collisions*, edited by R. Bock, Vol. **3** (North Holland, 1982) p. 1.
11. L. Palafox, Dissertation, Cranfield University, 1997.
12. A.N. Ostrowski, S. Cherubini, T. Davinson, D. Groombridge, A.M. Laird, A. Musumarra, A. Ninane, A. di Pietro, A.C. Shotter, and P.J. Woods, submitted to Nucl. Instrum. Methods Phys. Res. A.
13. R.B. Firestone (Editor), *Table of Isotopes* (John Wiley & Sons, New York, 1996).
14. L.M. Solin, Yu.A. Nemilov, V.N. Kuz'min, and K.I. Zharebtsova, Yad. Fiz. **29**, 289 (1979).
15. G. Schrieder, A. Müller-Arnke, and A. Richter, Nucl. Phys. A **279**, 463 (1977).